

LETTER TO THE EDITOR

# Optical QPOs with different periodicities in CSS and ZTF light curves of the quasar 4C 50.43

GuiLin Liao<sup>1</sup>, XingQian Chen<sup>1</sup>, PeiZhen Cheng<sup>1</sup>, Xue-Guang Zhang<sup>1\*</sup>

Guangxi Key Laboratory for Relativistic Astrophysics, School of Physical Science and Technology, GuangXi University, No. 100, Daxue Road, Nanning, 530004, P. R. China e-mail: xgzhang@gxu.edu.cn

## ABSTRACT

Long-standing optical quasi-periodic oscillations (QPOs) with periodicity of hundreds to thousands of days have been accepted as indicators for central sub-pc binary black hole systems (BBHs) in broad line active galactic nuclei (BLAGN). However, there are so far no direct reports on whether such reported optical QPOs have their periodicities constant in different periods. Here, based on different methods applied to light curves of 4C 50.43 in different periods, optical QPOs with periodicity of 1124days was detected in the CSS V-band light curve, while a shorter periodicity of 513days was detected in the ZTF *g/r* band light curves. Despite the two periodicities near-harmonic 2:1 ratio, their absence of simultaneous detection in the lomb-scargle periodograms of the ZTF light curves suggests that they are unlikely to be harmonically related. Potential factors were considered to explain these two distinct periodicities, especially different temporal coverage, signal-to-noise ratio and time steps between the CSS and ZTF light curves, as well as the effects of red noises related to intrinsic AGN variability. Our analysis shows that red noises have strong influence on the different periodicities in 4C 50.43 supporting our previous simulations. The results in this manuscript strongly indicate that it should be cautioned for applications of determined optical QPOs in BLAGN having strong intrinsic AGN variability.

**Key words.** galaxies:active - galaxies:nuclei - quasars:supermassive black holes

## 1. Introduction

Long-standing optical quasi-periodic oscillations (QPOs) observed in long-term light curves of broad line active galactic nuclei (BLAGN) have been proposed as potential indirect indicator of central sub-pc binary black hole systems (BBHs). Through applications of detected optical QPOs with periodicities ranging from hundreds to thousands of days, over 200 sub-pc BBHs candidates have been reported. Large-scale time-domain surveys identified 111 potential candidates in Graham et al. (2015b) and confirmed 50 quasars exhibiting significant QPOs in Charisi et al. (2016). For studies of individual sources, PG 1302-102 exhibits periodicity of about 1800days (Graham et al. 2015a), PSO J334.2028+01.4075 shows periodicity of 542days (Liu et al. 2015), while SDSS J015910.05+010514.5 (Zheng et al. 2016) and SDSS J025214.67-002813.7 (Liao et al. 2021) display periodicities of 1500days and 1607day, respectively. Compelling cases have also been found in Nearby AGN, such as Mrk 915 with 1150day QPOs (Serafinelli et al. 2020) and Mrk 231 with 1.2year QPOs (Kovacevic et al. 2020). In addition, our recent works have reported several optical QPOs: 6.4year QPOs in SDSS J0752 (Zhang 2022a), 3.8year QPOs in SDSS J1321 (Zhang 2022b), 340day QPOs in SDSS J1609 (Zhang 2023a), 1000day QPOs in SDSS J1257 (Zhang 2023b), and 550day QPOs in the quasar PG 1411+442 (Zhang 2025b).

However, the authenticity of the QPOs remains controversial, although these studies provide important indirect evidence for the existence of sub-pc BBHs. Red noises related to intrinsic AGN variability may produce similar periodic features as first discussed in Vaughan et al. (2016) and in our recent works in Zhang (2023a,b); Liao et al (2025); Zhang (2025a). Moreover, the effects of intrinsic AGN variability on the detected optical

QPOs, especially whether it may cause the detected QPOs to significantly deviate from the real intrinsic QPOs, has not been discussed in depth. Our recent simulation study tackled this question in Zhang (2025b) that in 41.52% of simulated light curves created in sub-pc BBHs, the detected QPOs deviated significantly from the input orbital period, often being less than two to four times the orbital period.

Although we (Zhang 2025b) have proposed that AGN variability may affect the periodicity of QPOs, there are no relevant examples that can directly support this hypothesis. In this manuscript, we report on a distinctive source, 4C 50.43, identified as a candidate of sub-pc BBH with an optical QPOs that have a reliable periodicity of about 1125days confirmed by Graham et al. (2015b) based on the Catalina Sky Survey (CSS). However, a significantly shorter periodicity of about 513days is detected in its optical light curves collected from Zwicky Transient Facility (ZTF) (Bellm et al. 2019; Dekany et al. 2020). It is the first time to report such periodicity discrepancy of optical QPOs in different periods. The structure of this manuscript is as follows: Section 2 presents the analysis of optical QPOs in both CSS and ZTF light curves; Section 3 discusses the possible explanations for the periodicity discrepancy; and Section 4 summarizes the main conclusions. Throughout the manuscript, we have adopted the cosmological parameters of  $H_0=70 \text{ km s}^{-1} \text{ Mpc}^{-1}$ ,  $\Omega_m=0.3$ , and  $\Omega_\Lambda=0.7$ .

## 2. Optical QPOs in 4C 50.43

The CSS V-band light curve of 4C 50.43 with MJD-53000 from 505 to 4505 (May 2005 to April 2016) and the ZTF *g/r* band light curves with MJD-53000 from 5204 to 7489 (March 2018 to June 2024) were collected and shown in top panels of Fig. 1. Here, the

arXiv:2603.09275v1 [astro-ph.GA] 10 Mar 2026

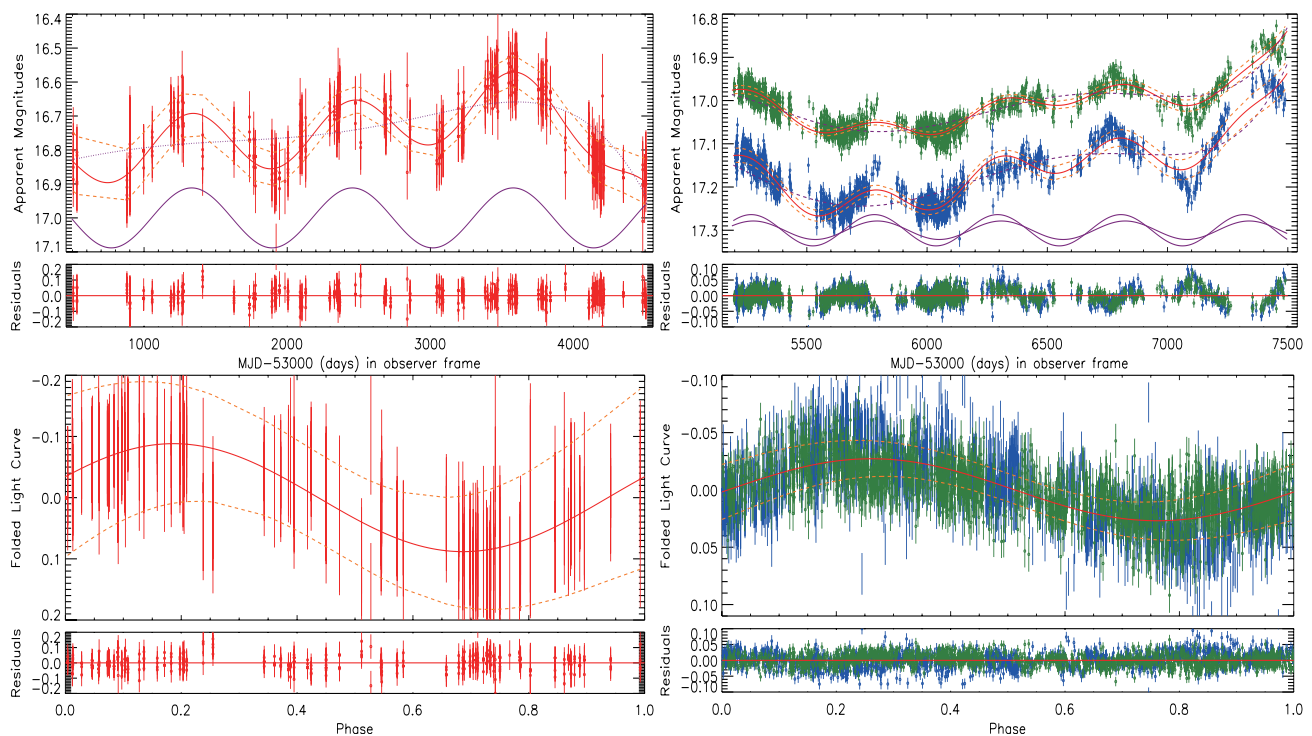


**Fig. 1.** Light curves fitting result of the CSS-V band (left, red symbols) and the ZTF *g/r* band (right, blue and green symbols). The first row presents the direct sinusoidal fitting results: in top panel, the solid red lines and orange dashed lines show the best-fitting results and corresponding  $5\sigma$  confidence bands from a sinusoidal function plus a fifth-degree polynomial component. The dashed purple lines represent the polynomial components, and the solid purple line represent the determined sinusoidal components. The second row show the phase-folded fitting results: in top panel, the solid red lines and dashed orange lines show the best-fitting results and the corresponding  $5\sigma$  confidence bands. The bottom panels of each row display the corresponding residuals (light curves minus the best fitting results), with solid red line showing residuals=0.

ZTF-*i* band light curve is not considered, as it contains relatively few data points. To improve the accuracy and reliability of optical QPOs, the direct fitting method, the phase-folding method, and the generalized Lomb-Scargle (GLS) method (VanderPlas 2018) have been applied.

The collected light curves are described by using a direct sinusoidal fitting approach that incorporates both long-term trend by a fifth-degree polynomial and periodic sinusoidal component. Here, the sinusoidal function is only used to model the periodic structure in the light curves, and does not involve discussions of physical origin of QPOs. Through the Levenberg-Marquardt least squares technique, the best fitting results can be determined and are shown in top panels of Fig. 1, with  $\chi^2/\text{dof} \sim 0.4$  and determined periodicity  $1122 \pm 24$  days in the CSS V-band light curve, and with  $\chi^2/\text{dof} \sim 1.9$  and determined periodicity  $512 \pm 16$  days in the ZTF *g/r*-band light curves.

Further, after subtracting the polynomial components, the light curves are phase-folded based on the determined periodicity. A sinusoidal function is then applied to describe the folded light curves, and the fitting results are shown in bottom panels of Fig. 1 with  $\chi^2/\text{dof} \sim 0.4$  for the folded CSS-V band light curve and  $\chi^2/\text{dof} \sim 2.1$  for the folded ZTF *g/r* band light curves.

In order to check the robustness of the QPOs, GLS method is employed. Top panel of Fig. 2 presents the GLS powers of the light curves. A significant peak at approximately 1125 days is detected in the CSS-V band (solid red line), while the ZTF *g/r* bands (solid lines in blue and in green, respectively) exhibit prominent peaks around 515 days. All detected primary peaks exceed the  $5\sigma$  significance level (false alarm probability  $\text{FAP}=3e-7$ ), as determined by the Bootstrap method.

The uncertainty associated with the GLS determined periodicity is defined as half the full width at half maximum of the distribution of the peak periodicity obtained through bootstrap resampling within 1000 loops. Specifically, the original light curve is resampled 1000 times, with each resampled set randomly selecting more than half of the original data points. The bootstrap method determined distributions of the periodicities are shown in middle and bottom panels of Fig. 2.

QPOs with periodicities of  $1122 \pm 24$  days and  $512 \pm 16$  days were detected in the CSS-V band and the ZTF *g/r* band light curves, using both the direct method and the phase-folded method. Similar periodicities of  $1125 \pm 40$  days and  $515 \pm 4$  days were also identified using the GLS method. The consistency of these results across different methods reinforces the reliability of the findings, collectively suggesting the presence of a significant QPOs with periodicity of around  $1124 \pm 64$  days in the CSS-V band, consistent with that reported by Graham et al. (2015b). While the ZTF *g/r* band show a periodicity of around  $513 \pm 20$  days, it apparently differs from the one detected in the CSS-V band. Although the ratio of the two periodicities exhibits a near integer multiple of 2 relationship, the absence of simultaneous significant peaks around 1125 days in the GLS periodogram (Fig. 2) of the ZTF *g/r* bands suggests a lack of harmonic coherence.

Before ending the section, the probability of optical QPOs in 4C 50.43 related to intrinsic AGN variability (red noises) can be simply determined. The intrinsic AGN variability was simulated using the Continuous AutoRegressive (CAR) process (Kelly, Bechtold & Siemiginowska 2009):

$$dLMC_t = \frac{-1}{\tau} LMC_t dt + \sigma_c \sqrt{dt} \epsilon(t) + b dt, \quad (1)$$

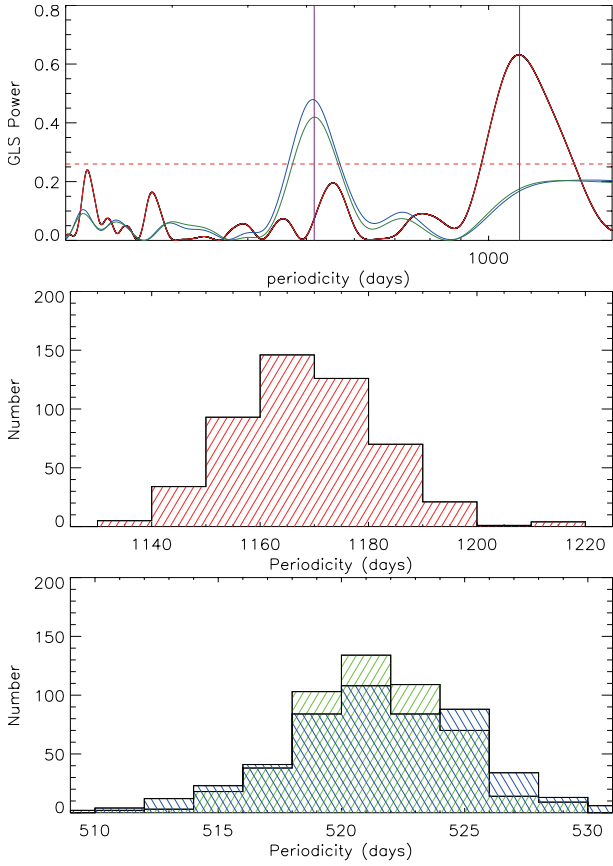


**Fig. 2.** Top panel shows the GLS periodograms of light curves. Solid lines in red, blue, and green show the corresponding results from the CSS V-band and ZTF r/g-band light curves. The horizontal dashed lines in red indicate the corresponding  $5\sigma$  significance level ( $FAP = 3e-7$ ). Middle and bottom panels show distributions of the periodicity determined by the bootstrap method from the CSS V-band light curve and the ZTF g/r-band light curves.

where  $\epsilon(t)$  denotes a white noise process with zero mean and unit variance. The mean magnitude  $bd$  was sampled from the typical range of 16 to 19 mag for low-redshift quasars. The relaxation timescale  $\tau$  was randomly selected within the range of 100 to 1000 days, in line with typical quasar values reported in Kelly, Bechtold & Siemiginowska (2009); MacLeod et al. (2010). The parameter  $\frac{\tau \times \sigma^2}{2}$ , which corresponds to the variances of simulated light curves, was randomly sampled within the typical range of variance values in the ZTF light curves of SDSS quasars, from 0.001 to 0.32. The uncertainties  $LMC_{err}$  of the simulated light curves  $LMC$  are determined based on the relative uncertainties in the observed light curves,  $\frac{LMC_{err}}{LMC} = \frac{LMC_{obs.err}}{LMC_{obs}}$ . The time information  $t = [t_{css}, t_{ztf}]$  is the combined time information of CSS V-band and ZTF g-band light curves of 4C 50.43. Then, among  $1e6$  simulated light curves, there are 113 light curves collected according to the following criteria. The GLS determined periodicity in the simulated light curve with  $t = t_{css}$  ( $t = t_{ztf}$ ) should be larger than 1124-128days (513-80days) and smaller than 1124+128days (513+80days) and have the corresponding peak value in the GLS powers higher than 0.5 (0.4) (the peak values larger than 0.6 and 0.5 in CSS and ZTF in 4C 50.43). Therefore, the probability should be 99.99% ( $1-113/1e6$ ), the corresponding confidence level higher than  $4\sigma$ , that the detected optical QPOs in 4C 50.43 are not from intrinsic AGN variability.

### 3. Potential causes of QPOs detection inconsistencies between CSS-V and ZTF g/r band

Given the significant wavelength overlap between the CSS-V and ZTF g/r bands, both probe similar regions of the accretion disk. The periodicity discrepancy is therefore unlikely to reflect radial dependence; instead, it is more likely attributable to red noise, as well as variations in S/N, temporal coverage, and time steps between the CSS and ZTF light curves.

As detailed discussions in our recent work Zhang (2025a), the effects of intrinsic AGN variability should be accepted to explain the periodicity discrepancy of optical QPOs in different wavelength bands in different periods in 4C 50.43. Here, an additional oversimplified method is applied to re-check the effects of red noises related to intrinsic AGN variability. The intrinsic AGN variability (red noises) was similarly simulated by the CAR process, but with time information to be  $t_{ztf}$  of the ZTF g-band light curve of 4C 50.43. And then the intrinsic QPOs was introduced into the red-noise-dominated light curves in the form of a sinusoidal function  $S(t) = A \times \sin \frac{2\pi t}{T}$  with amplitude  $A$  randomly selected from the set [0.1, 0.2, 0.3, 0.4, 0.5, 0.6, 0.7, 0.8, 0.9, 1, 2, 3, 4, 5, 6, 7, 8, 9] multiplied by the variance of the red noise. The periodicity  $T$  is randomly selected from 300days to 700days. The simulated light curves including QPOs and intrinsic AGN variability can be created by  $S(t) + LMC_t$ .

Based on the above method, a total of 50000 light curves were generated with the same information  $t$  as the ZTF g band light curve of 4C 50.43 (including the observation timestamps and temporal sampling), due to its high quality. The corresponding periodicities of these simulated light curves were detected using the GLS method. Upper left panel of Fig. 3 presents the distribution of the ratio of the intrinsic periodicity  $T$  to the measured periodicity  $T_o$  (with a significance level exceeding  $5\sigma$ ) derived from the simulation light curves using the GLS method. The results indicate that the majority of the ratios are inconsistent with 1, leading the influence of red noises on the intrinsic QPOs to be apparent. Meanwhile, among the 50000 simulated light curves, 37152 exhibited a periodicity ratio  $T/T_o \leq 1.5$ . Meanwhile 3042 showed substantial deviations, with some ratios reaching up to 4, suggesting that red noises significantly affects the accuracy of periodicity measurements. The remaining light curves were excluded from the statistical analysis due to the lack of statistically significant periodicity. The results strongly indicates that effects of red noises can be applied to naturally explain the periodicity discrepancy in 4C 50.43.

Considering the temporal coverage of the ZTF light curves may not be sufficient to detect the 1124days periodicity with statistical significance. Five light curves with time spans similar to that of the ZTF g band were randomly selected based on the existing CSS-V band light curves. The time spans of these light curves are 2236days, 2475days, 2217days, 2208days, and 2466days, with the corresponding data points being 152, 220, 138, 154, and 226, and sampling frequencies of 0.068, 0.089, 0.062, 0.07, and 0.09 respectively. GLS analysis was then performed on each of these light curves, with the results shown in upper right panel of Fig. 3.

The analysis reveals that QPOs in all five light curves are concentrated around 1124days, indicating that such time spans are sufficient for identifying this periodicity. Furthermore, higher sampling frequencies yield more significant detection of the 1124days QPO, while reducing the significance of the 513day periodicity. Given that the ZTF light curves possess comparable temporal coverage and sampling frequencies, the 1124days pe-

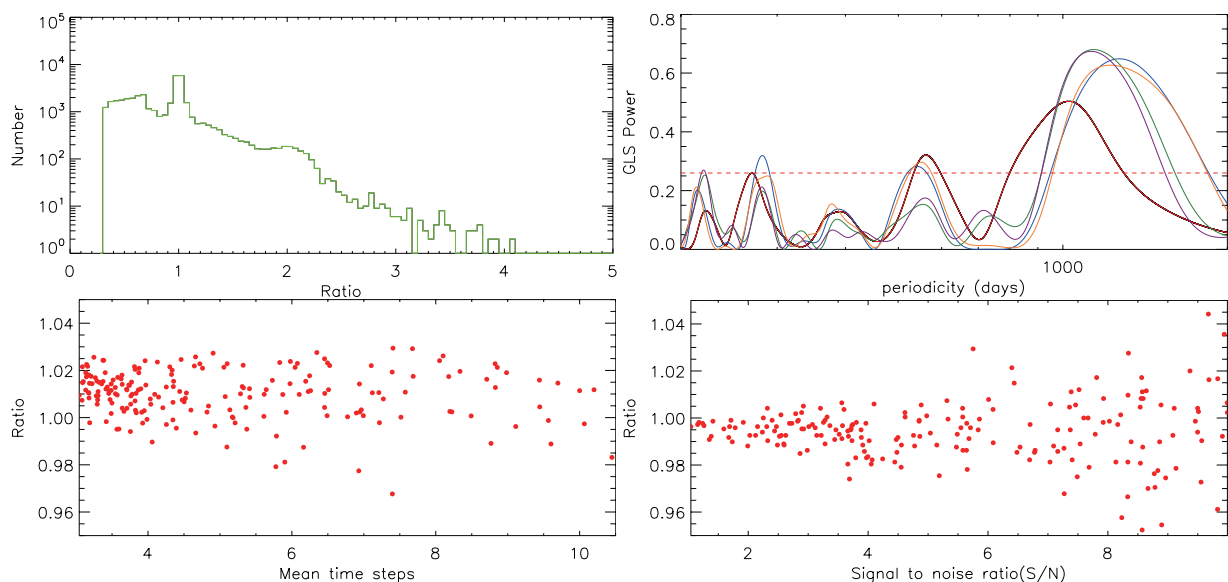


**Fig. 3.** Upper left panel shows distribution of the ratio of the periodicity  $T$  to the measured periodicity detected by GLS method applied in the simulated light curves including sine component and intrinsic AGN variability. Upper right panel shows the GLS periodograms of five light curves randomly selected from the CSS V-band light curves, with time spans 2236days, 2475days, 2217days, 2208days, and 2466days (in orange, green, red, blue, and purple, respectively), similar to that of the ZTF g band. Lower left and right panels show periodicity ratios between each subset with varying time steps (lower left) and varying signal-to-noise ratios (lower right) and the original ZTF g band light curve.

periodicity should be detectable if it were truly present. However, the ZTF light curves exhibit a dominant peak at 513days with no significant detection at 1124days. Therefore, the absence of the 1124days periodicity in the ZTF light curves cannot be attributed to insufficient temporal coverage; rather, this periodicity likely does not exist in the ZTF.

Due to the smaller time steps and higher signal-to-noise (S/N) ratios of ZTF light curves than CSS light curves, it is necessary to check whether quality of light curves can be applied to explain the detected periodicity discrepancy in 4C 50.43, especially effects of time steps and signal-to-noise ratios.

For effects of the time steps, 200 subsets containing 1/6 to 3/4 of the original data points were randomly selected from the ZTF g-band light curve of 4C 50.43. For effects of the S/N, the original photometric uncertainties were scaled by randomly selected factors between 1 and 10 and added to the ZTF g-band light curve of 4C 50.43, with this process repeated 200 times. The periodicities of both two sets of samples was determined by GLS method, and the resulting periodicities were compared to that of the original light curve in terms of their ratio. As shown in the bottom panels of Fig. 3, the results reveal that variations in time steps have only a limited impact on QPOs detection, with the periodicity remaining largely consistent with that of the original ZTF g-band light curve of 4C 50.43. Meanwhile, there were also few effects of S/Ns on detected periodicities, leading to only around 5% difference between intrinsic periodicities and determined values. Therefore, quality of light curves has few effects on the detected periodicity discrepancy in 4C 50.43.

## 4. CONCLUSIONS

We report the quasar 4C 50.43 exhibiting a significant discrepancy in periodicity of optical QPOs that is unlikely to represent a harmonic relationship: 1124days in the CSS Vband and 513days in the ZTF g/r bands, as revealed by different methods. Through simulations by CAR process, confidence level higher than  $4\sigma$  can be confirmed that the detected optical QPOs in 4C 50.43 are not

related to intrinsic AGN variability. Several possible mechanisms were considered to explain this difference, such as different temporal coverage and quality of light curves, as well as the effects of red noises. In conclusion, the periodicity difference is more likely caused by intrinsic AGN variability. At current stage, although the unique periodicity discrepancy only reported in 4C 50.43, the results in the manuscript strongly indicate it should be cautioned for applications of optical QPOs in BLAGN especially having strong intrinsic variability leading to detected periodicity very different from intrinsic values.

*Acknowledgements.* The authors gratefully acknowledge the anonymous referee for giving us constructive comments to greatly improve the paper. Zhang gratefully acknowledges the kind grant support from NSFC-12373014 and 12173020 and the support from Guangxi Talent Programme (Highland of Innovation Talents). This paper has made use of the data from ZTF and CSS, and the MPFIT package, and the NASA/IPAC Extragalactic Database (NED).

## References

- Bellm, E. C.; Kulkarni, S. R.; Barlow, T.; et al., 2019, PASP, 131, 068003  
 Charisi, M.; Bartos, I.; Haiman, Z.; et al., 2016, MNRAS, 463, 2145  
 Dekany, R.; Smith, R. M.; Riddle, R.; et al., 2020, PASP, 132, 038001  
 Graham, M. J.; Djorgovski, S. G.; Stern, D.; et al., 2015a, Natur, 518, 74  
 Graham, M. J.; Djorgovski, S. G.; Stern, D.; et al., 2015b, MNRAS, 453, 1562  
 Kovacevic, A. B.; Yi, T. F.; Dai, X. Y.; et al., 2020, MNRAS, 494, 4069  
 Kell B. C.; Bechtold J.; Siemiginowska A., 2009, APJ, 698, 895  
 Liu, T. T.; Gezari, S.; Heinis, S.; et al., 2015, ApJL, 803, L16  
 Liao, W. T.; Chen, Y. C.; Liu, X.; et al., 2021, MNRAS, 500, 4025  
 Liao, G. L., Chen, X. Q., Zheng Q., Liu, Y. L., Zhang, X. G., 2025, A&A, 698, 265  
 MacLeod C. L., et al., 2010, APJ, 721, 1014  
 Serafinelli, R.; Severgnini, P.; Braitto, V.; et al., 2020, ApJ, 902, 10  
 VanderPlas, J. T., 2018, ApJS, 236, 16  
 Vaughan, S.; Uttley, P.; Markowitz, A. G.; et al. 2016, MNRAS, 461, 3145  
 Zheng, Z. Y.; Butler, N. R.; Shen, Y.; et al., 2016, APJ, 827, 56  
 Zhang X. G., 2023a, MNRAS, 525, 335.  
 Zhang X. G., 2022a, MNRAS, 512, 1003  
 Zhang X. G., 2023b, MNRAS, 526, 1588.  
 Zhang X. G., 2022b, MNRAS, 516, 3650.  
 Zhang, X. G. 2025a, ApJ, 979, 147  
 Zhang X. G., 2025b, ApJ, 983, 90